Geometry into the Dendritic Faulting and Thrust patterns

Dr. N.L. Dongre

Fault segment of the San Andreas dendritic faults.: Vertical strokes define the linear extent of a fracture; fractures with greater length release more energy. Evanescent persistent clusters can be identified. After a long time this pattern is replaced by lattice-wide periodic fractures. The dendritic nature of the network of secondary faults associate with plate boundaries and a possibly tegular character of the space between elements of the network.

Abstract--Momentum dissipation methods may provide a useful way to examine mountain- building processes. Here, forward models of crustal deformation are presented in which faults form along paths that minimize the total (frictional and gravitational) work associated with slip. The numerical model produces thrust wedges analogous to the wedges produced by viscous models but with explicit fault paths rather than diffuse internal deformation. The model reproduces the general geometry of real compression belts, highlighting the basic competition between friction and topography (gravitational work) which may drive the evolution of orogenic zones. In particular, it was observed that Dendritic Faulting System as a geologic features. While some modeled features differ from observations, the results suggest that for many applications momentum dissipation may be a good approximation for macro scale crustal deformation.

1. Introduction

While there exist an infinite number of ways for the Earth's crust to deform under compression, Real Mountain belts display only a small subset of these deformations. The structural geometry of compression orogens appears to be characteristic: a few large fault zones root into the hinterland basement, while a greater number splay toward the surface in an imbricate fan structure, commonly rooted in a shallow decollement.

Dr. N.L. Dongre
Jaypee Nagar Rewa (M.P.) 486450

Nearly all active faults are observed to dip toward the hinterland, and the age of fault formation tends to become younger with increasing distance from the hinterland. The fact that compressional belts worldwide typically show these same features indicates that this style reflects the fundamental mechanics of continental deformation (*Molnar and Lyon-Caen*, 1988; *Cook and Varsek,* 1994).

The obvious dependence of mountain topography on fault geometry suggests an analysis based on the formation and evolution of discrete fault paths, rather than on viscous or plastic flow fields (e.g., *Chapple,* 1978; *England and McKenzie,* 1982; *Willet et al.,* 1993). While viscous and plastic models can generate displacement or velocity fields analogous to the deformation occurring in mountain belts, momentum transport in these models is by definition diffusive. Accordingly, these models cannot evolve discrete fault planes directly comparable to those forming real mountain structures.

As an alternative, in this paper it was considered that path-based models using the hypothesis of minimum work. In my modeling, slip occurs along the fault path through the crust that involves the least mechanical work out of all possible paths. While the mathematical foundation of momentum dissipation modeling lacks the rigor of more conventional force balance modeling, previous efforts have shown this approach to be a good approximation for specific eodynamical systems, including thrust systems (*Mitra and Boyer*, 1986; *Molnar and Lyon-Caen,* 1988; *Kleinrock and Morgan,* 1988), and the conceptual simplicity of the approach is certainly attractive. In this paper, the aim is to examine critically the characteristics of momentum dissipation mountain belts, comparing these characteristics to those found in real organs. It is begun by reviewing past use of models in geophysics and then proceed to discuss analytical and numerical models for mountain building.

2. Minimum-Work Techniques in Geodynamics

The use of minimization principles within the Earth sciences has a long and controversial history. Minimum work and minimum dissipation are examples of variational principles, which suppose that the minimization or maximization of some quantity (e.g., work) over the entire physical system will replicate the dynamics given by conventional Newtonian analysis. For a variety of simple physical systems, minimum-dissipation techniques can be proven mathematically to be correct, in that they always yield unique flow, velocity, or deformation fields identical to those obtained from solutions to classical force-balance equations or electric field equations. Examples of these systems include simple elastic bodies [*Saada,* 1974], slow viscous (Stokes) flow [*Lamb,* 1945], and the distribution of current in electrical circuits [*Feynman* et al., 1965].

For more complex, nonlinear systems, it is often impossible to prove analytically a correspondence between variational and Newtonian principles or to identify a unique variational function to be minimized or maximized [*Finlayson and Scriven*, 1967]. Bird and Yuen [1979] used this fact to argue that minimum-dissipation techniques for predicting the orientation of spreading ridges and transforms were invalid and should not be invoked. Specifically, they . argued that mantle convection depends strongly on body forces, features acoupling between momentum and thermal transport, and occurs within vaguely defined boundaries, which, taken together, mathematically precluded the identification of an appropriate variational function. Thus they argued againsthe use of variational principles for modeling most realistic geological systems.

While the mathematical analysis of Bird and Yuen [1979] has not been questioned, the scope of their conclusions has been. As noted by Sleep et al. [1979], the fact that variational principles applied to geologic systems lack a mathematically rigorous basis does not necessarily imply that they are poor approximations. Sleep et al. [1979] went on to show that, for the particular case of ridge-transform systems, the problems identified by Bird and Yuen [1979] could be reasonably neglected and reiterated the basic conclusion that models based on minimizing dissipation yielded results comparable to those based on force-balance analysis. This conclusion was verified by Kleinrock and Morgan [1988], who suggested that the success of the minimum-dissipation technique derived from the fact that plate boundaries minimizing dissipation also minimized resistive forces.

Accordingly, while it is clearly not appropriate to invoke minimization principles a priori to justify geological modeling, them remains the possibility that minimum-work models may produce good approximations for particular applications. A number of authors have already invoked minimum-work arguments to investigate specific aspects of mountain building. In examining foreland duplexes, Mitra and Boyer [1986] used minimization of work as the major criterion for partitioning

slip between existing ramps and the creation of new thrusts. Similarly, Jamison [1993] qualitatively invoked work minimization to discuss the evolution of triangle zones in fold-thrust belts. Molnar and Lyon-Caen [1988] suggested that the lateral expansion of continental plateaus primarily resulted from a need to minimize the gravitational work associated with uplifting existing topography, though they neglected the frictional work associated with deformation and did not explicitly address the evolution of the fault systems within the mountain belt. The model presented here differs from these previous applications in that it presents a complete, forward model for orogenic-scale deformation

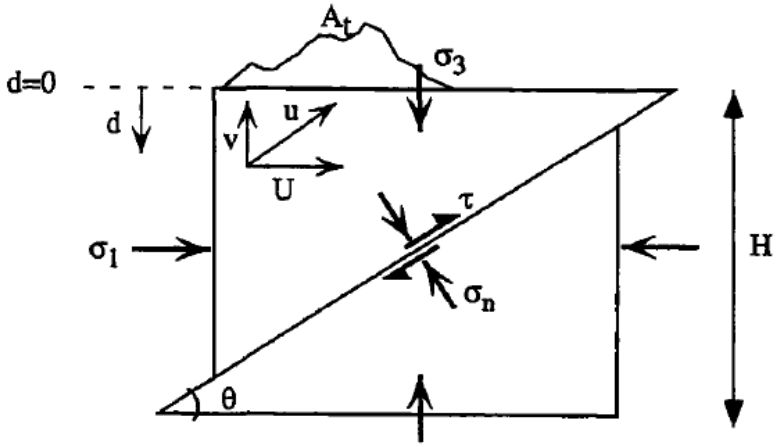

Figure 1. Detail of a portion of fault path, showing geometry and stress variables as discussed in text (Jeffrey and Christopher, 1998).

3. Analytical Model: Application to Anderson's Theory

The *Anderson* (1905) theory of fault formation remains the principal explanation for observed fault geometries. This theory supposes a pair of rigid blocks, separated by a fault dipping at some angle θ (Figure 1). The vertical principal stress is taken as $\sigma_3 = \rho_c g d$,and the horizontal principal stress as $\sigma_1 = \sigma_3 + \Delta\sigma_{xx}$,where. $\Delta\sigma_{xx}$ is the tectonic driving stress causing compressional strain, ρ_c is the density of the crust, g is the acceleration due to gravity and d is depth. The resolution of the principal stresses on the dipping plane into normal $(\sigma_n)$and shear (τ)components is given by

$$\sigma_n = \frac{\sigma_1+\sigma_3}{2} - \frac{\sigma_1-\sigma_3}{2}\cos 2\theta \tag{1}$$

$$= \rho_c g d + \frac{\Delta\sigma_{xx}}{2}[1 - \cos 2\theta]$$

$$\tau = -\frac{1}{2}(\sigma_1 - \sigma_3)\sin 2\theta = -\frac{\Delta\sigma_{xx}}{2}\sin 2\theta \tag{2}$$

For static friction, it is appropriate to use Amonton's Law, in which the shear stress is related to the normal stress by

$$|\tau| = \mu[\sigma_n - \lambda\sigma_3]_c g A v = -\rho_c g U \tan\theta \tag{3}$$

Where λ the ratio of pore fluid pressure to Iithostatici spressure (the Hubbert-Rubey fluid pressure ratio) and μ isthe frictional coefficient of dry rock (Suppe, 1985).Substituting (1) and (2) into (3) gives a relation between the tectonic driving stress .$\Delta\sigma_{xx}$and the angle of the fault, θ

$$\Delta\sigma_{xx} = \frac{2\mu(1-\lambda)\rho_c g U}{\pm\sin 2\theta - \mu(1-\cos 2\theta)} \tag{4}$$

Anderson (1905) supposed that the correct fault geometry was that which required the dissipation value of $\Delta\sigma_{xx}$Setting $d\Delta\sigma_{xx} I d\theta = 0$ gives the relation

$$\tan 2\theta = \pm(1/\mu) \tag{5}$$

where the positive tangent reflects compression and the negative tangent reflects extension. For values of μ ranging from 0.10 to 0.80, (5) predicts compressive (thrust) fault dips of 25°-40°, in reasonable agreement with observed fault geometries (Turcotte and Schubert, 1982).

Here it is expressed that the Anderson theory in terms of minimum dissipation. The frictional dissipation rate along the fault is given by

$$W_f = u\tau A_f \tag{6}$$

where$u$ is the velocity along the fault, τ is the stress along the fault, and A_f is the fault area. From Figure 1, it maybe seen that

$$u = \frac{U}{cos\theta} \tag{7}$$

$$A_f = \frac{H}{\mathrm{Sin}\theta} \tag{8}$$

where U is the horizontal shortening velocity, $H$is the thickness of the block, and $A_f$has been expressed per unitlength into the plane of the section. For given values of $\mu$and θ, $\Delta\sigma_{xx}$may be found from equation (4) and τmay befound by substituting $\Delta\sigma_{xx}$into equation (2). The resulting frictional dissipation is thus equal to

$$W_f = -\frac{1}{2}UH\Delta\sigma_{xx}\left[\frac{sin2\theta}{sin\theta cos\theta}\right] = -UH\Delta\sigma_{xx} \tag{9}$$

In other words, the rate of work is proportional to and will be dissipation at the same angle θas the tectonic drivingstress $\Delta\sigma_{xx.}$thus the least work approach predicts the same fault geometry as the Anderson theory (Figure 2). It is worth noting that the angular dependence of the Anderson theory is only recovered when all terms in the dissipation equation (6) are included. For example, the resolved shear stress itself has an entirely different angular dependence and, in fact, has no dissipation in the range of $\theta = 0^{\circ}$ to 90°

It can be extended that the least-work approach to include the gravitational work associated with lifting topographic loads, which was not considered in the original Anderson theory. For the geometry shown in Figure I, the gravitational rate of work (per unit length into the section) is given by

$$W_{\mathrm{g}} = \rho_c \mathrm{g}Av = -\rho_c \mathrm{g}\left[\frac{H^2}{2\tan\theta} + A_t\right] U\tan\theta \tag{10}$$

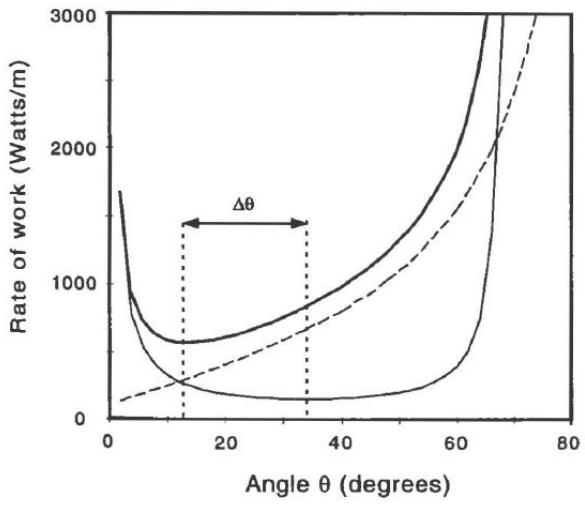

Figure 2. Rate of work as function of fault angle for geometry shown in Figure 1. Total rate of work (bold, solid line) is the sum of frictional dissipation (fine, Solid line) and gravitational work (dashed line). $\Delta\theta$ Represents the change in the Momentum dissipation fault angle resulting from the addition of gravitational work to the original Anderson theory for this case, $\mu = 0.40, A_l$= 1000 $\mathbf{km^2}$• $\rho_\iota = 2700, kg/m^3$ $U = 1$ cm/yr, and $H = 10$ km.

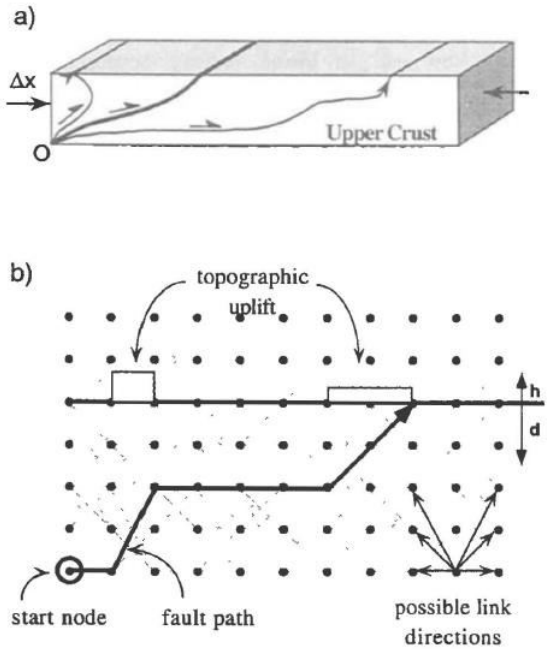

Figure 3. (a) Schematic of momentum dissipation model, in which slip always occurs along the path through the crust satisfying the condition of minimum total (path-integrated) work. (b) Example model grid, with 10 × 5 nodes and six exit directions from each node. Thin arrows in lower right show allowed exit directions from each node; thick arrow indicates a fault path through the grid; white areas show topographic uplift resulting from this path (Jeffrey and Christipher ,1998).

where A is the total cross-sectional area being lifted. $A,$ is the cross-sectional area of the topography above $d = 0,$ and v is the vertical component of the velocity. The total work involved in deformation is the sum of (9) and (10). Including the gravitational work component forces faults to form at shallower angles (by the amount $\Delta\theta$ in Figure 2) to compensate for the extra gravitational work penalty. Essentially, the total momentum dissipation trajectory compromises between high frictional and high gravitational work to minimize the sum (Figure 2). This balance between friction and gravity forms one of the major themes of section 4.

4. Description of Numerical Model

The numerical model consists of a two-dimensional cross section through the crust, represented as a Cartesian grid of nodes in a vertical plane (Figure 3). The crust between the right and left boundaries is considered to shorten an increment Δx (= 160 m) per time step. and this shortening is accommodated at each time step by the formation of a thorough going fault. Allowable ("candidate") fault paths are formed by linking nodes subject to the constraints that (1) fault trajectories must always start at a single, fixed node on the lower boundary, (2) fault trajectories may only cut horizontally or upward, never down, and (3) fault trajectories must exit the upper surface of the grid. Constraint mandates a single point from which all fault paths must originate. This constraint is identical to the geometry of a physical sandbox model, where all faults must eventually meet the junction between the backstop and the lower, moving boundary. In accordance with constraint 2, each node has several possible "exit" directions that the fault trajectory may follow to nodes in adjacent grid columns, ranging counter clockwise from 0° (horizontal, right) to 180° (horizontal, left) (Figure 3b).

For each candidate trajectory through the grid, work is calculated as the path integral of gravitational, frictional, and (optionally) internal deformation work terms, and the path with the momentum total dissipation is chosen as the actual fault for that time step. For a given node-to-node segment of a path, gravitational work (W_{g}) is

$$W_{\mathrm{g}} = \int_{-d}^{h} F_{\mathrm{g}}.\, dx = \rho_c A_h \mathrm{g}\,(d+h)\Delta x \sin(\theta) \qquad (11)$$

where F_g is the force due to gravity, dr is the displacement vector for that segment, d is the depth below sea level ofthe node, h is the height of the topography above sea level over that node, ρ_c is the average crustal density, g is the acceleration due to gravity, θ is the dip of the fault segment, and A_h is the area of the fault plane segment projected onto the horizontal plane. In all cases, there is no topography present at initiation of the model $(h(x) = 0)$.

The frictional work (W_f) for each node-to-node segment is calculated as

$$W_f = \tau A_f \Delta_x \tag{12}$$

where τ is the shear stress across the fault surface and A_f is the area of the fault plane. For simplicity, it is assumed that all shortening (Δx) is transferred to slip along each fault segment. It is assumed that a vertical principal stress$\sigma_3 = \rho_g(d + h)$and a horizontal principal stress $\sigma_1 = \sigma_3 + \Delta\sigma_{xx\prime}$, where $\Delta\sigma_{xx\prime}$, is fixed for all fault segments as 1×10^8Pa. The shear stress is calculated from the principle stresses as described above.

At each time step, a recursion algorithm evaluates the dissipation associated with all possible fault paths through the grid, and the path with the minimum work is selected as the actual fault path for that time step. Topography is then incremented above ramps in the chosen path by an amount $\Delta h = \Delta x \sin\theta/|\cos\theta|$,where the cosθ term corrects for mass "lost" by treating uplift in a vertical column over the fault segment, rather than explicitly calculating kink axes. Since the new topography changes the gravitational work configuration for the next time step, the momentum dissipation path may change as well. This results in a dynamic model, in which the topographic evolution is tightly coupled to the evolution of fault paths. Only one fault path is chosen at each time step, although superimposing faults from a short series of time steps gives a better idea of the complete range of active faults during any period. For simplicity, it is not deformed or translated the grid (or any prior fault paths) during the "deformation."

In these experiments, a 30-km-thick section of crust is deformed, implicitly treating both ductile deformation within the lower crust and brittle deformation within the upper crust as Momentum dissipation phenomena. At least one study has suggested that plastic deformation can be treated via dissipation techniques (*Chung and Richmond*, 1993), and there is an intuitive analogy between the yield strength of a plastic material and the frictional strength of a sliding surface. Moreover, the important characteristics of the model results do not depend on the overall crustal thickness and would be the same if a thinner crustal section is chosen. While it is acknowledged that this treatment could be a source of error in the results, the purpose here is to test a simplified model for the entire mountain-building process.

5. Results of Numerical Modeling

Results of the numerical modeling are presented as several case examples, moving from simple cases in which fault paths are relatively unconstrained to more complex cases in which additional dissipation terms and geologic preconditions strongly constrain allowable fault paths.

5.1. Sandbox Model

The simplest configuration of the model has only a uniform friction coefficient, includes no dissipation due to internal deformation (bending), and includes no strain weakening through time. In many respects, this simple model is analogous to particulate "sandbox" models in that the system has no memory of where slip has previously occurred. This "sandbox" model illustrates a central point, that evolution of the synthetic mountain belts fundamentally reflects the competition between gravitational and frictional dissipation (Figure 4). Faults initially choose short, direct paths to the surface to minimize path length, and thus frictional dissipation (Figure 4a). However, as topographic uplift ensues, faults prefer longer paths which avoid uplifting existing topography and hence reduce gravitational dissipation (Figures 4b and 4c). This competition results in a topographic wedge, analogous to the viscous or Coulomb wedges reported by others (*Daviset at*., 1983; *Dahlen, 1984*; *Willet et ai*., 1993). Faults continually make minor adjustments at depth to minimize the sum of friction and gravity, forming a smooth topographic profile (*Win Tsuang*., 2012). The exact number of ramps and flats varies with the shortening increment chosen for the model (160 m here); smaller

increments allow the model to more precisely tune the fault geometry, producing more "braids" in the fault plane. Nevertheless, the topographic evolution of the wedge and the general character of the fault zone 00 not depend on the chosen shortening increment.

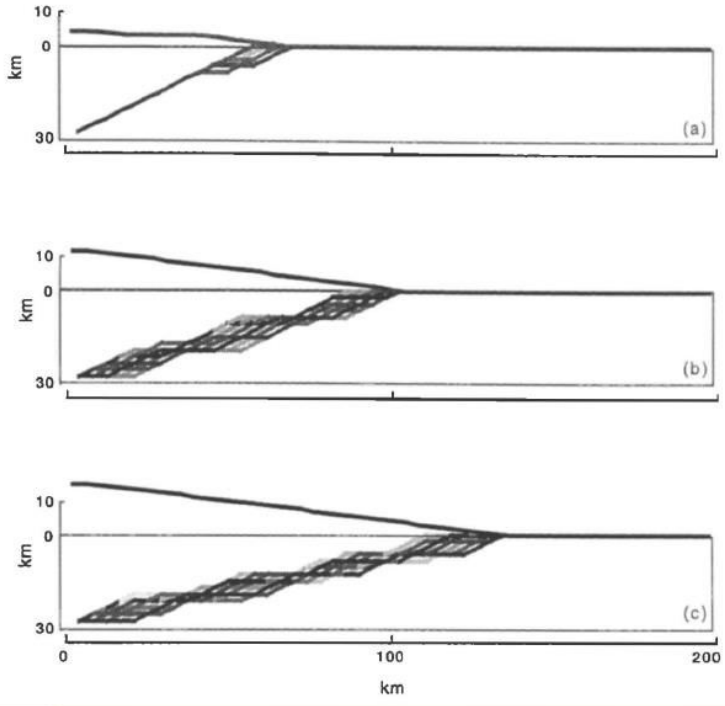

Figure 4. Simple "sandbox" model evolution for a uniform crustal friction of ~ = 0.20. In each case, least work fault paths from the preceding 20 time steps are shown, with darker shading representing the more recent paths. In all cases, the initial crustal section was 30 km x 200 km. with a vertical node spacing of 2 km. a horizontal node spacing of 4 km. and eight possible node-to-node link directions. The Hubbert-Rubey ratio has been assumed to be 0.37. The shortening increment for each time step was 160 m; assuming a nominal shortening rate of 1 cm/yr, each time step represents 16,000 years: (a) 40 time steps. (b) 140 time steps. (c) 240 time steps.

Since published estimates for friction coefficients in fault zones vary widely (*Byerlee,* 1977, *Logan and Rauenzahn*, 1987*; Mount and Suppe*, 1987; *Bird and Kong,* 1994), it is tested that a range of values for μ, from 0.05 to 0.8.Increasing the coefficient of friction results in an increased dissipation penalty for long fault paths, forcing a steeper topographic slope (Figure 5a). It is found that reasonable wedge slopes (less than -15°) are possible only with low friction coefficients (less than 0.40). These coefficients are much lower than that of 0.85 found by *Byerlee(*1978),although they agree with published values for the San Andreas system (*Mount* and *Suppe,* 1987; Bird and Kong.1994) and experimental results on fault gouge (*Logan and Rauenzahn*, 1987).

It should be noted that unlike the Coulomb wedge of *Dahlen* (1984), the minimum-dissipation wedge is not self-similar. While the topographic slope of the wedge is constant during growth the fault system (when averaged over a few time steps) approximates a plane leading from the nucleation point to the deformation front. Accordingly the average dip of the fault paths becomes shallower through time, and the taper angle (topographic slope plus fault dip) also decreases. In section 5.5 it was offered that a simulation with a fixed decollement horizon which allows a direct, quantitative comparison with the Coulomb critical wedge theory.

The amount of dissipation required to accomplish shortening increases through time. While the first fault path requires 2.0 x 10^{15} J/M of work the 200th requires 3.7 × 10^{15} J/M. where both figures are calculated per unit length into the plane of the section (Figure 5b). The higher work figure represents a power expenditure of -7500 W/m assuming a convergence velocity of 1 cm/yr or an expenditure of 35.000 Wlmfor a 5-cm/yr convergence velocity. .

5.2 Internal Deformation

Following *Mitra and Boyer* (1986), it can also be included dissipation due to internal deformation. Calculated as the dissipation involved in the flexural slip of the hanging wall as it passes

through a kink axis (i.e., bend in the fault rejectory). As derived by *Mitra and Boyer* (1986), the shear strain involved in moving across a kink axis is$\gamma = 2\,tan\,(a/2)$ where a is the change in fault trajectory across the bend. Thus the node-to-node dissipation involved in this shearing is

$$W_i = \bar{\tau}\,\gamma \mathrm{v} = \tau\gamma(d+h)\Delta x \qquad (13)$$

where $V$the volume of rock transported across the kink axis and $\tau$is the average shear stress involved in flexural slip (e.g .• the shear stress as calculated above, evaluated at half the depth to the fault).

The simplest results presented above are constrained only by gravity and friction, and the fault patterns form perfectly smooth topography as these terms are continually balanced. In contrast, including the work due to internal deformation constrains faults to paths that also minimize the number of bends in the fault trajectory (Figure 6a). While the resulting topography still takes the form of a wedge with the same average slope-versus-friction dependence, the geometric pattern of faulting is quite different, with long, straight fault segments imbricating the entire crust, and the topography has a rougher, stepped profile.

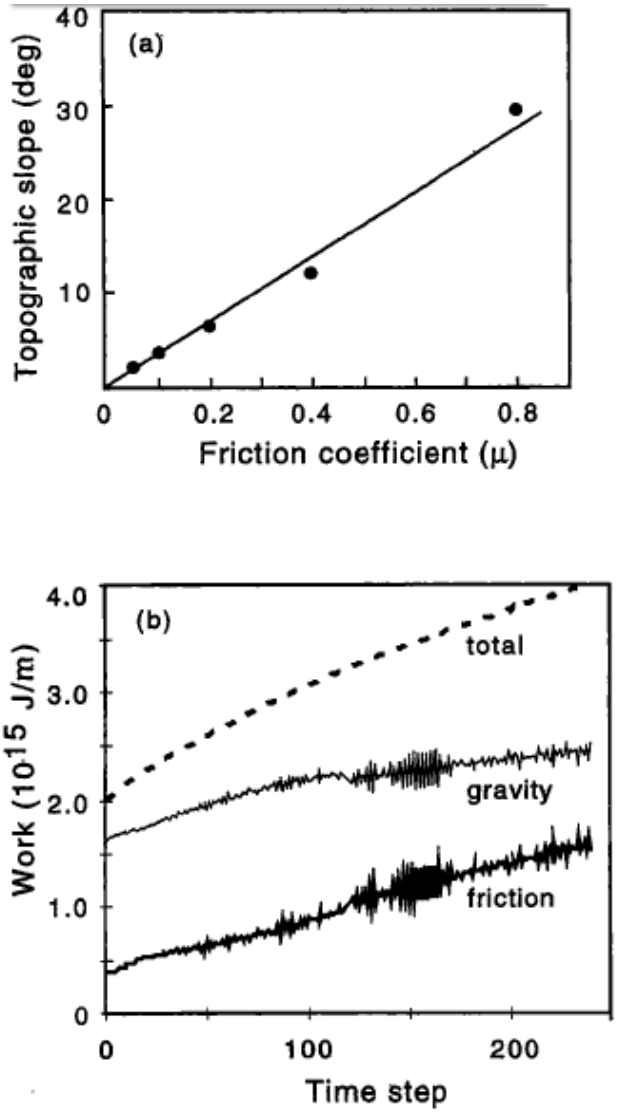

Figure 5. Dynamics of the model shown in Figure 4. (a) Dependence of topographic slope on friction coefficient (μ.). (b) Gravitational dissipation (fine solid line), frictional dissipation (thick solid line), and total dissipation (dashed line) to accomplish shortening through time.

5.3. Isostasy

Isotactic compensation affects the distribution of dissipation during mountain building (Molnar and Lyon-Caen, 1988).From a momentum dissipation perspective, the effects of isostasy are twofold. First, for fixed amount of crustal thickening, the formation of an isostatic crustal root requires a smaller in Crease in potential energy than in the non isostatic case and thus less gravitational dissipation. Second since isostasy partitions much of the crustal shortening into the root, the buildup of topography is relatively slower. Both of these effects dissipation together to reduce the relative gravitational dissipation "penalty," causing the orientation of faults to be dominated by the frictional dissipation component.

In real mountain belts, compensation occurs regionally, over long wavelengths, and not locally. While the details of the recursion algorithm prohibit incorporating true regional compensation into this model, it was approximated that the effects by performing a column-by column Airy isostatic correction according to a prescribed compensation factor C(Turcotte and Schubert, 1982).

Given a node-to-node crustal thickening $(\Delta H = \Delta x \sin\theta/|cos\theta|)$, material was allocated to the crustal root (r)according to$\Delta_r = C\ \Delta H(\rho_c/\rho_m)$, where ρ_m is the density of the mantle and ρ_c is the density of the crust. The compensation factor (C) expresses the degree to which isostasy (buoyancy) rather than lithospheric strength supports topography, and ranges from 0 (for a rigid plate with no compensation) to 1.0 (for pure Airy isostasy). Appropriate values of C may be derived knowing the flexural rigidity and wavelength of loading (TurcottecniSchubert, 1982, p. 123). For a typical continental value of flexural rigidity $(10^{23} - 10^{24}\text{Nm})$and the wavelength of loading considered here (-100 km), values of $C < 0.5$ are appropriate.

Using this approximation, the model proves to be sensitive to isostasy. Compared to the non isostatic case, faults take shorter, more direct paths to the surface and create steeper topographic wedges (Figure 6b). Since compensation reduces the relative gravitational dissipation penalties associated with uplift, frictional penalties become more important. Faults respond by forming short paths that minimize frictional dissipation. Although the topography still takes the form of an orogenic wedge, it exhibits a steeper slope and advances much more slowly.

In reality, the degree of compensation should change during the evolution of mountain belts. Early stages of deformation result in narrow mountains largely supported by the rigidity of the lithosphere$(C \approx 0)$. As defonnation progresses and the mountain belt widens, the crustal root absorbs an increasing fraction of the thickening. As this occurs and as the compensation factor tends toward the Airy limit $(C \approx 1)$, frictional dissipation increasingly dominates the evolution of fault systems. As a result, it was predicted that narrow, under compensated mountain belts tend to expand laterally faster than wide, compensated mountain belts.

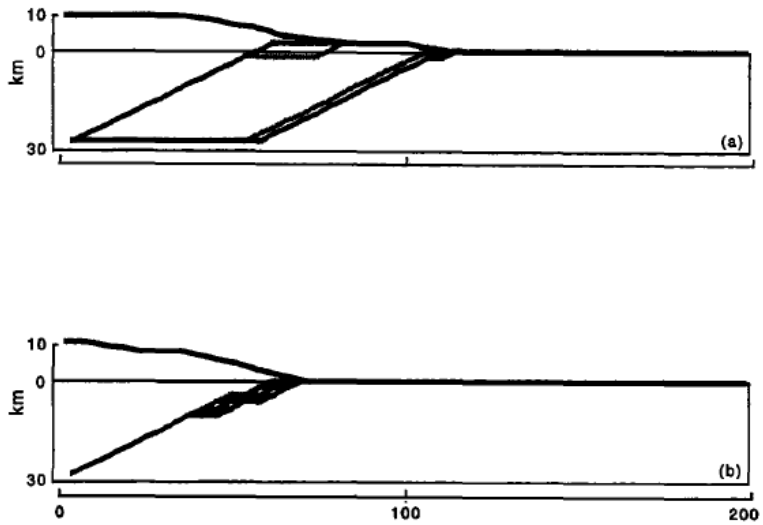

Figure 6.Example model results showing effects of, internal deformation and isostasy. (a) Same model configuration as Figure 4 but with addition of dissipation due to internal deformation, 140 time steps. (b) Same model configuration as Figure 4 but with addition of isostatic compensation$(C = 0.5)$, 200 time steps.

5.4. Strain Weakening

By allowing the friction coefficient to vary in space and time, various geological conditions can be simulated. First, real faults progressively weaken during slip, such that they have a "memory" of where slip has taken place. Although Coulomb wedge models often assume a pervasively faulted (Le., cohesion less) material, the observed reactivation of ancient structures in younger tectonic settings shows that old faults may became permanent zones of weakness compared with the surrounding rock matrix (*Goebel, Sammis, Backer, Dresen,and Schorlemmer*,2013). To approximate this in this model, there is option of including a simple strain weakening term, such that the effective friction coefficient of a segment that has previously slipped (μ'), is inversely proportional to the number of times that segment has slipped(N):

$$\mu' = \mu\left[w + \frac{(1-w)}{(1+N)}\right] \tag{14}$$

where w represents the asymptotic limit of the weakening factor as N gets large. With this addition, the model evolution depends on two parameters, $\mu$and w.

Without strain weakening, the model has no memory of where slip has occurred previously, and successive paths tend to form anastomosing zones rather than stable fault planes. The addition of the strain weakening term (14)results in "energy wells," paths that remain stable because of strain weakening and reduced friction, even after they are far from gravitationally optimal (Figure 7a). This results in fewer, more stable faults and a much rougher topography. In essence, paths no longer respond to slight topographic variations if the minimum dissipation involves continually slipping on an existing plane.

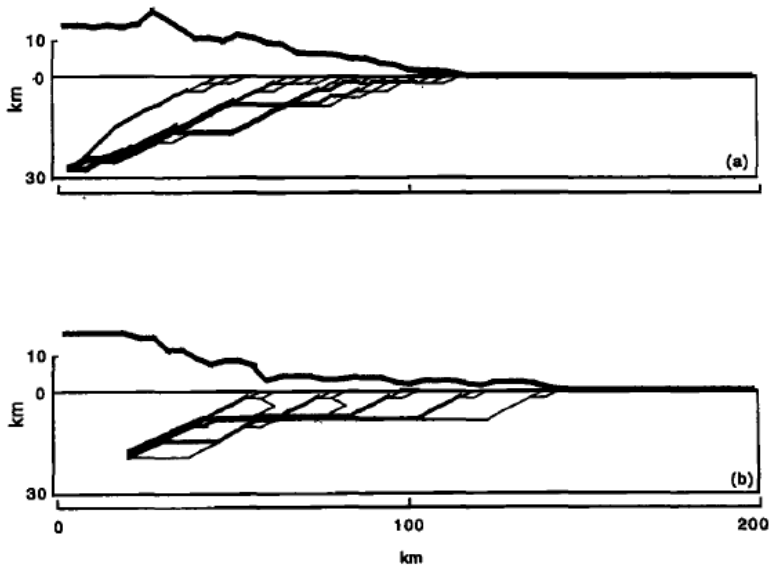

Figure 7. Model results for specific configurations discussed in the text. Here all faults have been shown, with line thickness scaled in proportion to the number of times that slip has occurred on that segment. Neither isostasy nor dissipation due to internal deformation has been included in these simulations. Elapsed time in each case is 220 time steps. (a) Inclusion of strain weakening, (b) Inclusion of low friction, weak layer at depth of 10 km and strain weakening.

5.5. Thin-skinned Thrusting

By placing a weak layer (friction coefficient reduction of 50%) at a depth of 10 Km, decollement formation and thin skinned thrusting can be simulated (Figure 7b). Faults that occur along the decollement experience lower average friction values than do the basement faults of the hinterland. The break in topographic slope at the boundary between the hinterland and foreland reflects this variation in average friction, with lower topographic slopes occurring over the weak decollement. Above the decollement, the regularly spaced surface breaks suggest the periodic valley ridge patterns observed in many foreland fold-thrust belts (Figure 7b). That this periodic structural style occurs only in the presence of a weak horizon suggests that the evolution of thin-skinned zones is markedly different from the evolution of basement thrusts.

The spacing of the faults in the thin-skinned wedge is proportional to the depth to the decollement. A similar relationship between decollement depth and fault spacing occurs in physical "sandbox" models of compressional wedges [*Liu et al*., 1992], with friction playing a subordinate role in controlling spacing (Figure 8a). Compared to this physical model, the minimum-work model displays a lower spacing-to-thickness ratio, probably reflecting steeper near-surface faults than those occurring in the sandbox model. A sample of fault spacings from the Pachmarhi is presented in Figure 8b. These examples have been restricted to cases where en echelon imbricates splay from a single decollement and a characteristic fault spacing can be observed. The distributionf spacings varies considerably among different fold-thrust belts but illustrates ageneral correlation between decollement depth and spacing. This relationship has also been found within individual thrust belts, where decollements step to shallower levels and thrust spacing decreases [e.g., *Price,* 1981].

The presence of a well-defined decollement permits a quantitative comparison with Coulomb critical wedge theory (*Davis et al*., 1983; *Dahlen*, 1984). As derived by *Dahlen* (1990), the approximate equation for the geometry of a cohesion less wedge at critical taper can be written as

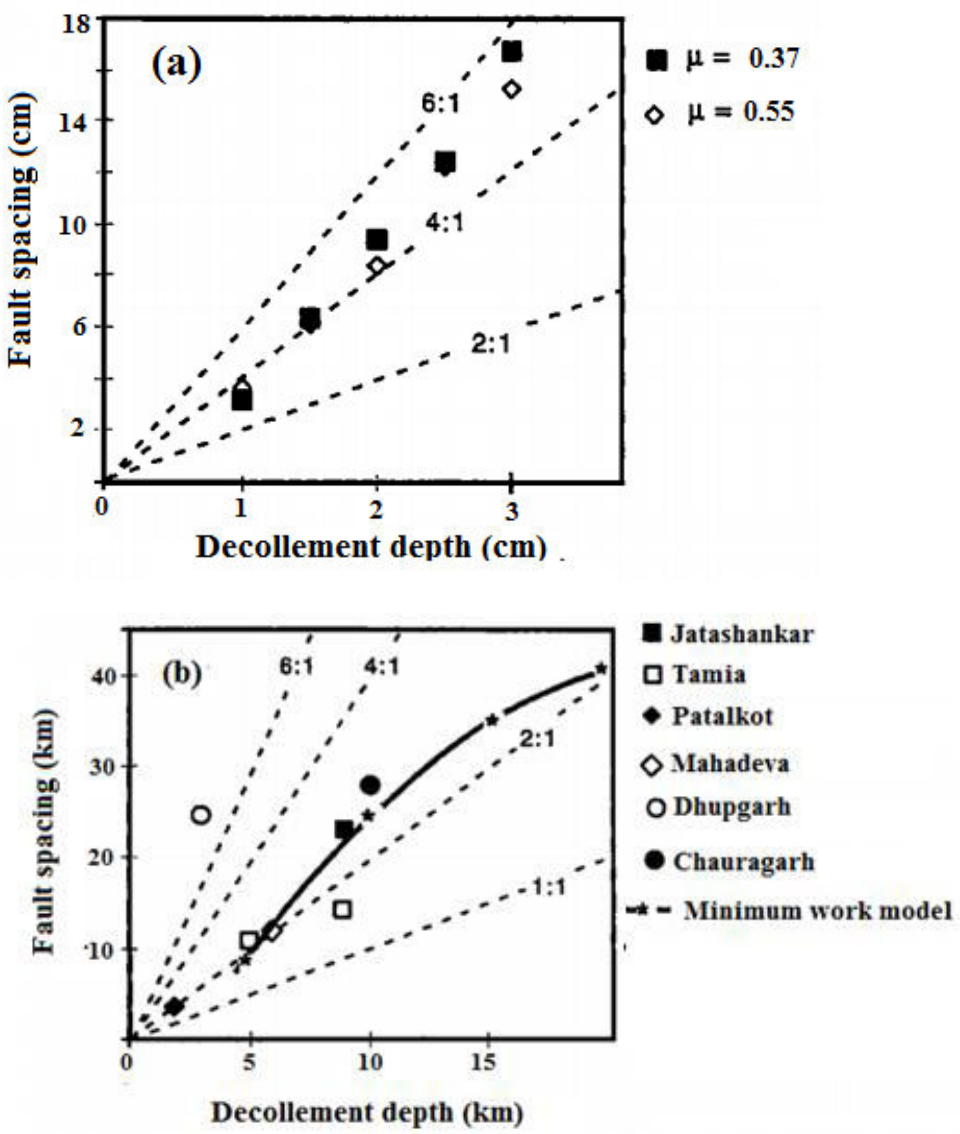

Figure 8. Spacing controlling in the Pachmarhi (India) region an example of momentum dissipation model

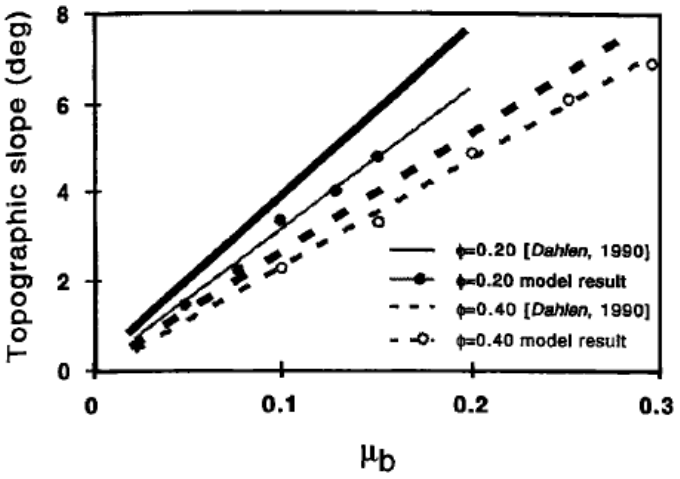

Figure 9. Quantitative comparison of minimum-work model with Coulomb critical wedge approximation of Dahlen (1990). In all cases, topographic slope $(\alpha\, in(15))$is plotted against basal friction coefficient (μ_b)Theoreticalresults from Dahlen(1990) are shown as bold lines; model results are shown as shaded data points and lines. Two sets of results are given: ϕ = arctan (0.20) (solid lines) and ϕ = arctan (O.40) (dashed lines).

$$a + \beta = (\mu_b + \beta)\left(\frac{1-\sin\phi}{1+\sin\phi}\right) \tag{15}$$

where a represents the topographic slope, β represents the dip of the basal decollement, μ_b, is the coefficient of frictionalong the basal decollement, and $\phi$is angle of internalfriction for the wedge. In this case, the decollement is flat (Figure 7b); corresponding to the case of $\beta = 0$. Satisfying this condition in (15) yields a linear relation between topographic slope and the basal friction coefficient (Figure9). Topographic slopes above the horizontal decollement in the dissipation model also exhibit a linear dependence on the basal friction coefficient and match the *Dahlen* (1990) approximation quite well (Figure 9).

Surface faulting patterns of the thin-skinned wedge shown interesting trend through time. During early evolution, fault paths constantly anastomose at depth, thickening all parts of the orogen "simultaneously," and thus producing a smoothly tapering wedge. During this period, the surface erupture (point where the fault path exits the top of the grid) migrates consistently toward the foreland. As thin-skinned deformation evolves, however, the surface rupture begins occasionally to jump backward, toward the hinterland (Figure 10). Thus, while out-of-sequence faulting is always present at depth in the orogen, only later-stage, thin-skinned deformation shows surface evidence of out of sequence motion.

One consequence of the valley-and-ridge topography is that back thrusts become possible (Figure 7b). Previously, with no strain weakening and smoothly tapered topography, paths that cut up and away from the high topography always involved less work than paths that cutup and toward the high topography (Figures 4a, 4b, and4c). Faults necessarily verged toward the foreland away from the high topography. With the inclusion of strain weakening, faults tend to choose the same path repeatedly, building a rougher topography with local depressions when faults do choose a new path, these depressions allow back thrusts to become _ gravitationally favorable. A similar association between forward verging thrusts and back thrusts is seen in the laboratory experiments of Liu et al(1992).

5.6. Effects of Erosion

Given the sensitivity of the least dissipation model to variations in topography, it is not surprising that erosion plays a major role in determining the structural geometry of the synthetic mountain belts. As an example, it was incorporated that an extremely simple erosion law, with the erosion rate proportional to the local slope of the topography multiplied by local stream flow (accumulated precipitation to the nearest drainage divide). This formulation, with erosion rate proportional to the stream power, has been used by a number of other investigators researching the erosion of orogens (Chase, 1992; Beaumont et at., 1992; Howard, 1994; Masek et aI.,

1994).Precipitation rate has been calculated by considering the change in saturation vapor pressure of air parcels lifted over the topographic profile (Masek et al., 1994). In this simulation, it was started fault trajectories from the middle of the grid and has applied the erosion law only to the right half of the grid. In essence, this duplicates the Orographic experiments of Beaumont et al. (1992).

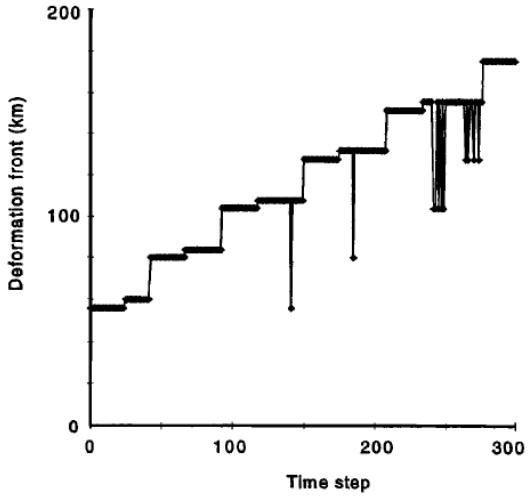

Figure 10. Deformation front (point where fault path exits upper surface of the grid) as a function of time for the thin-skinned model discussed in text and shown in Figure 7b. Note the out-of-sequence surface breaks which occur after -2 m.y.

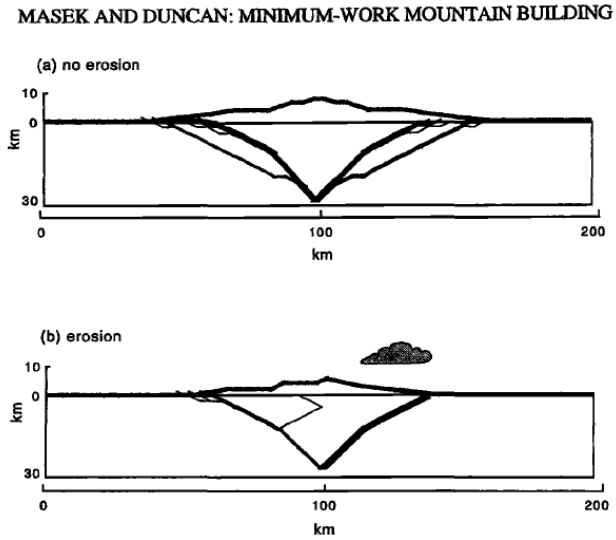

Figure.11. Effects of erosion on minimum-work model. (a) No erosion case, (b) The right half of the model experienced erosion (symbolized graphically by the orographic cloud), while the left half experienced no erosion. Both results show all fault paths up to time step 160, with line thickness scaled in proportion to the number of times that slip has occurred on that segment.

Since there is no random input into the model, the synthetic topography and deformation are symmetric about the central point without erosion (Figure 11a). With erosion, however, topography is continuously removed from the right half of the model, making that side gravitationally favorable for fault paths (Figure 11b).Deformation is thus concentrated on the side of the mountain belt experiencing erosion. With the particular erosion law used here, the mass efflux must eventually balance the tectonic mass influx, and the resulting mountain is in a steady state, with neither the topography nor the fault geometry changing significantly over time. These results are similar to those of *Beaumont* et al (1992), who found that the highest rates of rock uplift correlated with zones of intense precipitation and erosion. The results presented here further support the idea that surficial processes can play a role in affecting tectonic deformation (*Beaumont* et aI., 1992).

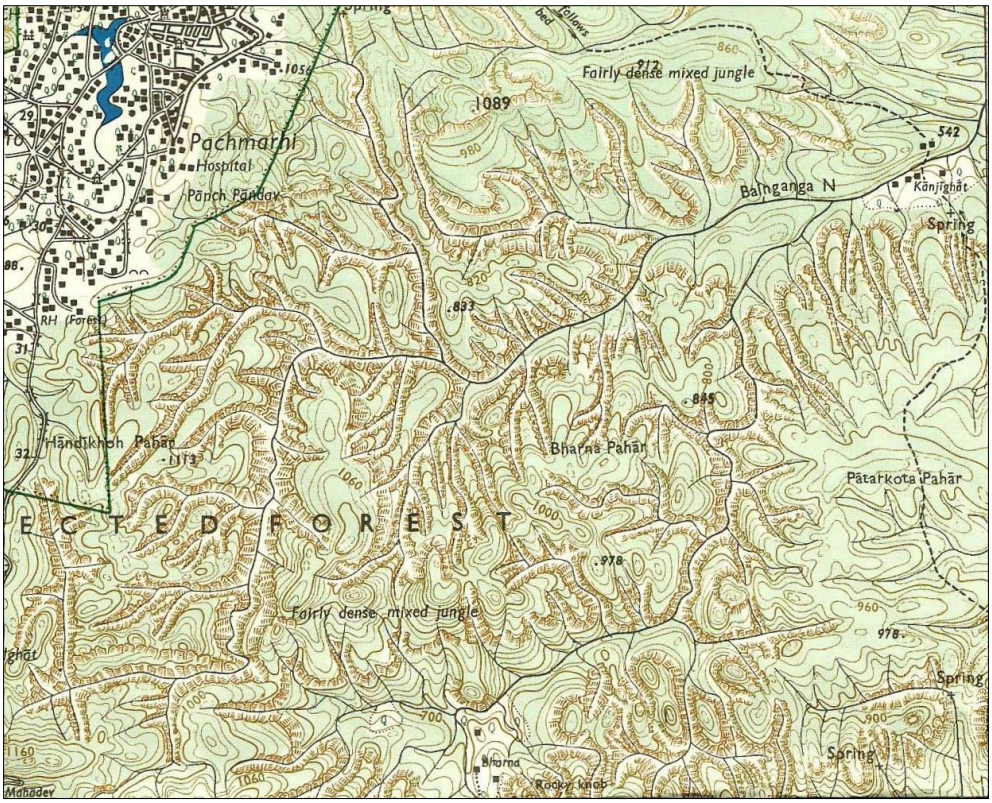

Figure 12.Momentum dissipation model reproduced significant character which is observed in the Pachmarhi, including the formation of dendritic faulting pattern. (Survey of India toposheet μ /7)

6. Discussion

The Momentum Dissipation model reproduces significant characteristics of observed tectonic belts, including the formation of dendritic faulting patterns (Figure 12), the development of thin-skinned thrust systems, and out-of-sequence thrusting. That the patterns of faulting formed by the model replicate these features suggests that mountain building approximates a minimum-work process at a crustal scale. However, other features of the simulated orogenic belts do not seem to agree well with observations. The inclusion of work due to bending, for example, leads to structural geometries that do not seem particularly realistic, and the model seems acutely sensitive to isostatic compensation. In addition, the partitioning between frictional and gravitational work within the model diverges from that found in the Pachmarhi for the Pachmarhi fold-thrust belt. While rational explanations for these discrepancies may exist within the context of minimum-work mechanics, they may also reflect fundamental shortcomings inherent in using approximate methods.

Now the study of the dendritic faulting turn to the observation of space time coupling of moments for the Pachmarhi, which has perhaps the best recent catalog compilation. It is more likely that the geological and seismological faults have separate populations. It is believed that the small events occur on the extension to smaller scales of the dendritic surface faulting associated with large-scale fracturing. Further it is suggestive that the braided character of the large faults on a scale less than 10 km is characteristic of those faults that extend from the surface to the bottom of the seismogenic zone, namely the large geologic faults. Thus the fault systems represent locations, as remarked, of complex boundaries that appear as a melange of highly damaged material, with the smaller-scale damage strongly influenced by the fractures of large scale. The magnitude-frequency law probably describes well the fractures on the small-scale micro features of the dendritic complex, and does not have an obvious bearing on the problems of rupture on the larger faults; the latter appear to have a different geometrical description.

Nevertheless, this model makes a number of interesting predictions that could be tested observationally. First, simulated back thrusts arise primarily from the gravitational effects of topographic depressions. While this effect would, in reality, be damped for deeply rooted faults; it should hold that shallow back thrusts are controlled primarily by existing topography. This prediction

could be tested using existing structural sections from actively deforming foreland belts. Second, it was consistently found that realistic fault geometries occur only with a weak friction coefficient, typically less than 0.40. As noted above, this is much lower than friction coefficients reported in laboratory tests. Finally, it is worth noting that the results replicate the findings of other researchers. Like *Beaumont et al.* (1992), it was found that erosion can strongly accelerate deformation, and like *DahLen* (1984) and *Chapple* (1978), a direct correlation observed between topographic slope and friction coefficient.

The model makes explicit the important role of topography in driving orogenic evolution. As mountain belts grow, continuing competition between gravitational work associated with lifting topography and frictional work associated with fault slip results in a wedge-like geometry. Relatively minor variations in friction and erosion act to perturb this balance, resulting in the rich variety of structural styles observed in mountain belts. The fact that this spectrum of structural styles can arise from a single, simple geodynamic model suggests that this approach may prove useful for studies of specific mountain systems. Finally, an interesting aspect of the minimum-work hypothesis is that faults behave as whole paths, such that local fault geometry is driven by the distribution of topography and friction over the entire fault, not just the local segment. Accordingly, local (e.g., field-scale) variability observed in structures may not just be "random "but may reflect a deterministic need to minimize work over much larger scales.

References

Allmendinger, R. W., D. Figueroa, D. Snyder, 1. Beer, C.Mpodozis, and B. L. Isacks (1990). Foreland Shorte ning and crustal balancing in the Andes at 30° S latitude, *Tectonics,* 9, 789-809,

Anderson, E. M. (1905), the dynamics of faulting, *Trans. Edinburgh Geol. Soc.,* 8, 387-402.

Baby, P., G. Herail, R. Salinas, and T. Sempere(1992), Geometry and kinematic evolution of passive roof duplexes deduced from cross section balancing: Example from the foreland thrust system of the southern Bolivian sub andeanzone, *Tectonics,* 11, 523-536,.

Barr, T. D., and F. A Dahlen (1988)., Thermodynamic efficiency of brittle frictional mountain building, *Science,* 242, 749-752,

Beaumont, C., P. Fullsack, and J. Hamilton (1992), Erosional control of active compressional orogens, in *Thrust Tectonics,* edited by K. R. McCLay, pp. 1-19, Chapman and Hall, New York,.

Bird, P., and X. Kong (1994), Computer simulations of California tectonics confirm very low strengths of major faults, *Geol.Soc. Am. Bull., 106,* 159-174,

Bird, P., and D. A Yuen (1979), the use of the minimum-dissipation principle in tectonophysics, *Earth Planet. Sci. Lett., 45,*214-217.

Byerlee, J. D. (1978), Friction of rocks, in *Experimental Studies of Rock Friction with Application to Earth quake Prediction,* edited by J. F. Evernden, pp. 55-77, U.S. Geological Survey, Menlo Park, Calif.,.

Chapple, W. M. (1978), Mechanics of thin-skinned fold-and-thrust belts, *Geol. Soc. Am. Bull.,* 89, 1189-1198,.

Chase, C. G. (1992), Fluvial lands culpting and the fractal dimension of topography, *Geomorphology,* 5, 39-57,.

Chung, K., and O. Richmond (1993), A deformation theory of plasticity based on minimum work paths, *Int. J. Plast., 9,*907-920,.

Cliff Ollier, Colin F. Pain – (2000) - The Origin of Mountains book.google.co.in

Cook, F. A, and J. L. Varsek (1994), Orogen-scale decollements, *Rev. Geophys., 32,* 37-60.

Dahlen, F. A (1984), Noncohesive critical Coulomb wedges: Anexact solution, *J. Geophys. Res.,* 89, 10,125-10, 133.

David G. Roberts, A. W. Bally – (2012) - Regional Geology and Tectonics: Phanerozoic Rift Systems book. google.co.in

Dahlen, F. A. (1990), Critical taper model of fold-and-thrust belts and accretionary wedges, *Ann. Rev. Earth and Planet. Sci., 18,* 55-99.

Davis, D.J. Suppe, and F. A. Dahlen (1983), Mechanics of fold-and thrust belts and accretionary wedges, *J. Geophys. Res., 88,* 1153-1172.

England, P., and D. McKenzie (1982), a thin viscous sheet model for continental deformation, *Geophys. J. R. Astron. Soc., 70,*295-321.

Feynman, R. P., R. B. Leighton, and M. Sands (1965), *the Feynman Lectures on Physics,* Addison-Wesley, Reading Mass.,

Finlayson, B. A., and L. E. Scriven (1967), on the search for variational principles, *Int. J. Heat Mass transfers, 10, 799-*

Froidevaux, C., and B. L. Isacks (1984), the mechanical state of the lithosphere in the Altiplano-Puna segment of the Andes, *Earth Planet. Sci. Lett., 71,* 305-314,

Gary Brierley, KirstieFryirs – (2008) - Geomorphology and River Management: Applications of the River book.google.co.in
Goebel, T.H.W, Sammis C.G, Backer, T.N. Dresen, G., and Schorlemmer. D., (2013) A Comparison of Seismicity Characteristics and fault structure between stick slip experiment and nature Pure appl. Geophys,
Howard, A. D., (1994) A detachment-limited model of drainage basin evolution, *Wat. Resour. Res., 30,* 2261-2285,
Jamison, W. R. (1993), Mechanical stability of the triangle zone: The back thrust wedge, *J. Geophys. Res.,* 98, 20,015-20, 030,
Jeffrey G. Masek, Christopher C. Duncan (1998) Minimum-work mountain building Papers on Geodesy and Gravity Tectonophysics DOI: 10.1029/97JB03213
John Grotzinger, Thomas H. Jordan, Frank Press – (2010) -Understanding Earth, book.google.co.in
Kleinrock, M. C., and J. P. Morgan (1988), Triple junction reorganization, *J. Geophys. Res.,* 93, 2981-2996,.
Lamb, H. (1945), *Hydrodynamics,* 738 pp., Dover, Mineola, N. Y.,.
Liu, H., K. R. McClay, and D. Powell (1992)., Physical models ofthrust wedges, in *Thrust Tectonics,* edited by K. R. McCLay,pp. 71-81, Chapman and Hall, New York,
Logan, J. M., and K. M. Rauenzahn(1987), Frictional dependence of gougemixutres of quartz and Mont Mori llonite on velocity, composition, and fabric, *Tectonophysics, 144, 87-108*,.
Masek, 1. G., B. L. Isacks, T. L. Gubbels, and E. J. Fielding (1994), Erosion and tectonics at the margins of continental plateaus, *J. Geophys. Res.,* 99, 13,941-13,956,.
McDougall, 1. W., and A. Hussain (1991), Fold and thrust propagationin the western Himalaya based on a Balanced cross sectionof the Surghar Range and Kohat Plateau, Pakistan, *MPGBull.,* 75, 463-478,.
Mitra, G., and S. Boyer (1986), Energy balance and deformation mechanisms of duplexes, *J. Struct. Geol.,* 8, 291-304.
Molnar, P., and H. Lyon-Caen (1988)., Some simple physical aspectsof the support, structure, and evolution of mountain belts ,in *Processes in Continental Lithospheric Deformation, Spec. Pap. Geol. Soc. Am.,* 218, 179-207,
Mount, V. *S.,* and J. Suppe (1987), State of stress near the San Andreas fault: Implications for wrench tectonics, *Geology,* 15, 1143-1146,.
Parfenov, L. M., A. V. Prokopiev, and V. V. (1995). Gaiduk, Cretaceous frontal thrusts of the Verkhoyansk fold belt,eastern Siberia, *Tectonics,* 14, 342-358,
Pascale Leturmy, Cécile Robin – (2010) - Tectonic and Stratigraphic Evolution of Zagros and Makran .book. google.co.in
Price, R. A. (1981), The Cordilleran foreland thrust and fold belt in thesouthern Canadian Rocky Mountains, in *Thrust and NappeTectonics,* edited by K. R. McClay and N. J. Price, *Geol.Soc. London, Spec. Pub.,* 9, 427-448.
Richard Huggett – (2011) - Fundamentals of Geomorphology book.google.co.in
Saada, A.S. (1974), *Elasticity Theory and Applications,* 643 pp., Pergamon, New York.
Schelling, D. (1992), The tectonostratigraphy and structure of the eastern Nepal Himalaya, *Tectonics, 925*-943.
Sleep, N. H., S. Stein, R. J. Geller, and R. G. Gordon (1979), Comment on "The use of the minimum-dissipat ion principle in tectonophysics" by P. Bird and D.A Yuen, *Earth Planet. Sci. Lett.,* 45, 218-220.
Suppe, J. (1985), *Principles of Structural Geology,* 537 pp., Prentice Hall, Englewood Cliffs, N. J.,.
Turcotte, D.L. (1982), and G. Schubert, *Geodynamics,* 450 pp., John Wiley, New York,
Willet, *S.,* C. Beaumont, and P. Fullsack, (1993) Mechanical model for the tectonics of doubly vergent Compres sion orogens,*Geology,* 21, 371-374,
William B. Bull – (2011) - Tectonically Active Landscapes books.google.co.in
Win-Tsuang Chi-yuen Wang (2012) Sequential thrusting model for mountain building: Constrain from geology and real-flow of Taiwan JGR Journal of Geophysical Research solid earth
Zoetemeijer, R., and W. Sassi, (1992) 2-D reconstruction of thrus tevolution using the fault-bend fold method, in *Thrust Tectonics,* edited by K. R. McCLay, pp. 133-140, Chapman and Hall, New York,